①

AUG 14 1961

325

814 61

NAA-SR-6047
COPY

MASTER

THERMAL EXPANSION
OF
SNAP MATERIALS

AEC Research and Development Report

ATOMICS INTERNATIONAL
A DIVISION OF NORTH AMERICAN AVIATION, INC.

251/8-14-61

DISCLAIMER

DISCLAIMER

Price $0.50
Available from the Office of Technical Services
Department of Commerce
Washington 25, D. C.

NAA-SR-6047
METALLURGY AND CERAMICS
23 PAGES

THERMAL EXPANSION OF SNAP MATERIALS

By
J. D. WATROUS

ATOMICS INTERNATIONAL
A DIVISION OF NORTH AMERICAN AVIATION, INC.
P.O. BOX 309 CANOGA PARK, CALIFORNIA

CONTRACT: AT(11-1)-GEN-8
ISSUED: JUL 30 1961

DISTRIBUTION

This report has been distributed according to the category "Metallurgy and Ceramics" as given in "Standard Distribution Lists for Unclassified Scientific and Technical Reports" TID-3400 (15th Ed.), August 1, 1959. A total of 600 copies was printed.

CONTENTS

Appendixes

TABLE

FIGURES

ABSTRACT

Thermal expansion characteristics were determined for the fuel-moderator, reflector, cladding, and engineering materials within the SNAP-2 core vessel. Values were determined for AISI Type 347 stainless steel, Hastelloy N, beryllium, zirconium, zirconium hydride, and zirconium-uranium hydrides, from room temperature to temperatures greater than 1300°F. Derived equations were calculated for these materials, using a least squares analysis.

Thermal expansion coefficients for the temperature range of 77 to 1200°F are: 10.34×10^{6} in./in.-°F, for Type 347 stainless steel; 7.46×10^{-6} in./in.-°F, for Hastelloy N; 9.07×10^{-6} in./in.-°F, for beryllium; and 6.12×10^{-6} in./in.-°F, for zirconium - 7 wt % uranium hydride with an $N_H = 6.4$.

I. INTRODUCTION

The coefficient of linear expansion as a function of temperature must be known for fuels, reflectors, cladding, and any other materials within the SNAP core vessel. Thermal expansion coefficients are used as the basis for stress calculations, during initial heating to temperature, operation at temperature, and subsequent cooling. Irradiation and hydrogen redistribution effects also cause stresses, during operating and thermal cycling.

Information concerning the thermal expansion of zirconium-uranium hydrides is unavailable in the literature. Values for stainless steel, Hastelloy N, and beryllium can be derived, from various sources, thereby presenting a possibility for variations in data reliability. It was decided to investigate the materials involved in the actual fuel element, to determine accurately the relative differences in thermal expansion characteristics.

II. EXPERIMENTAL APPARATUS AND PROCEDURES

The basic equipment consists of a null void volume quartz tube differential dilatometer, utilizing a linear variable differential transformer as a motion sensor. Figure 1 shows the essential parts of the dilatometer and accessory equipment.

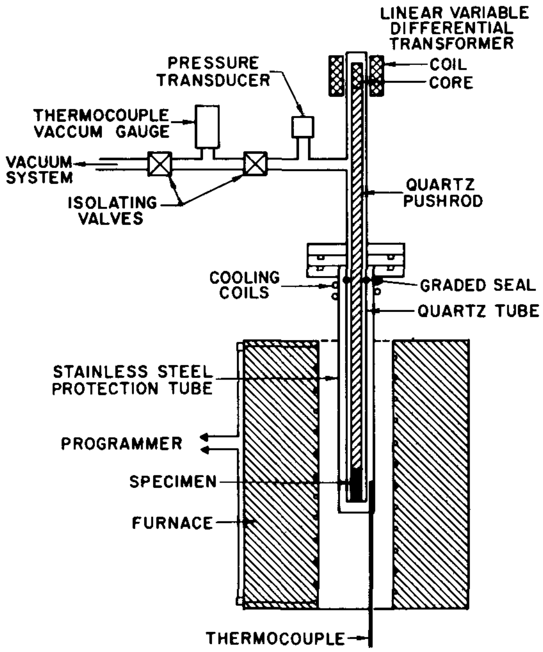

Figure 1. Quartz Tube Dilatometer

A vertically mounted resistance wound tube furnace is used to heat the specimen. The specimen rests on a quartz seat which is fused to a quartz tube. The tube is connected to a stainless steel flange by a graded seal, and the assembly is enclosed by a stainless steel protection tube. A quartz push rod rests on the sample, and transmits the motion of the sample to a linear variable differential transformer (LVDT) core located outside the furnace. A stainless steel (non-magnetic) protection sheath surrounds the push rod and transformer core. The LVDT coil is mounted outside the vacuum system, as shown in Figure 1. This upper assembly is air cooled, to prevent thermal expansion of the various components during a run.

The linear variable differential transformer consists of a magnetically susceptible core and three coaxial coils mounted on a ceramic coil form. Axial motion of the core produces an electrical potential which varies directly with the motion of the core. This signal is then bucked against a similar core-coil arrangement in a recorder, thereby producing a pen displacement which is linearly variable with the original core movement.

A programmed furnace control is used to obtain uniform heating rates with the saturable core reactor and resistance tube furnace. A two-pen recorder, for plotting both temperature and expansion, as functions of time, is used. For the hydride studies, pressure-sensitive transducers are used to measure the hydrogen dissociation pressures. These pressures are monitored on either manual or recording potentiometers.

A normal thermal expansion run consists of an initial evacuation period, leak checking, isolating the sample chamber, heating to a selected temperature, and cooling back to ambient. Evacuation to less than 5×10^{-3} mm was always achieved, accompanied by leak rates of less than 5×10^{-3} mm/hr into the system.

A heating rate of 3°C/min was selected, to allow complete heating and partial cooling during a normal working day. The programming system heated the specimen, at a rate of 2.8±0.2°C/min, to a selected temperature (from 700 to 900°C), where a manually operated switch reversed the system, allowing cooling at the same rate. One or more recorders followed both temperature and expansion, as functions of time. This information was then plotted, as expansion <u>vs</u> temperature, for further calculations.

III. MATERIALS

The Type 347 stainless steel was procured from normal commercial sources. The Hastelloy N rod was purchased from Haynes-Stellite Company, Kokomo, Indiana, suppliers of the reactor cladding material. Brush Beryllium Company, Cleveland, Ohio, supplied the reactor-grade hot pressed and extruded beryllium.

Reactor-grade zirconium was obtained from swaged crystal bar stock. For evaluation in the zirconium-hydrogen "delta" phase region, the zirconium was subsequently massively hydrided, as described in the literature.[1] Zirconium-uranium alloys were double arc melted, by the consumable electrode method, from reactor-grade zirconium and uranium pellets.[2] The ingots were subsequently extruded, swaged, annealed, and hydrided to various compositions for investigation. After hydriding, the specimens were ground to size, 0.240 to 0.250 in. in diameter. The length of the sample ranged from 1.3 to 2.2 in.

IV. DATA

Thermal expansion curves for zirconium - 7 wt % uranium are shown in Figure 2. Materials with H/Zr ratios of 1.70 to 1.80 appear to have identical expansion characteristics, while material with H/Zr = 1.57 expands at a slower rate.

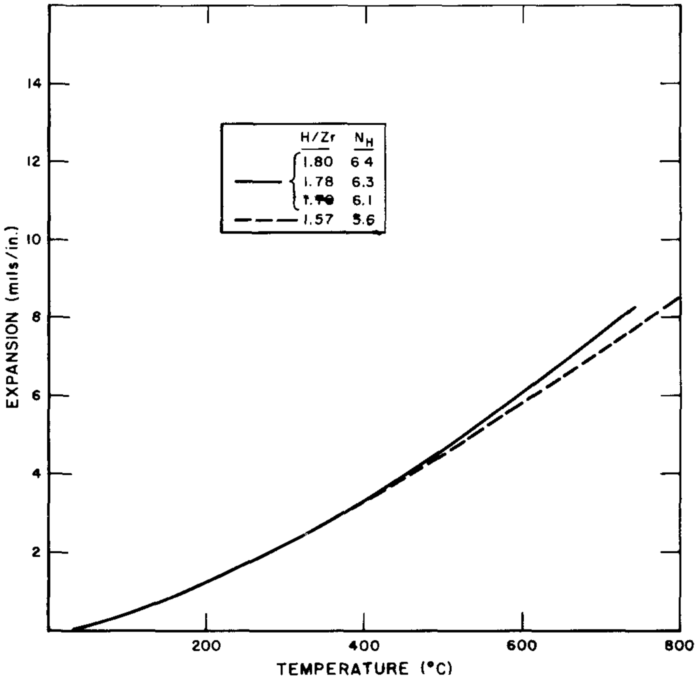

Figure 2. Thermal Expansion of Zirconium - 7 wt % Uranium Hydrides

This increase in the thermal expansion coefficient with increasing hydrogen content was also observed by Denver Research Institute,[3] in their studies on zirconium hydride. Figure 3 shows both the Denver Research Institute data and some data obtained on this project. Battelle Memorial Institute[1] obtained similar results, under more rapid heating conditions.

Claddings are required to be in close proximity with the fueled moderator material; thus, they must closely approximate the thermal expansion coefficient of the fuel. Curves obtained on Type 347 stainless steel are shown in Figure 4. The literature value[4] is plotted for comparison. It may be noted that the literature data originates at 0°C, while the present curves originate at 25°C.

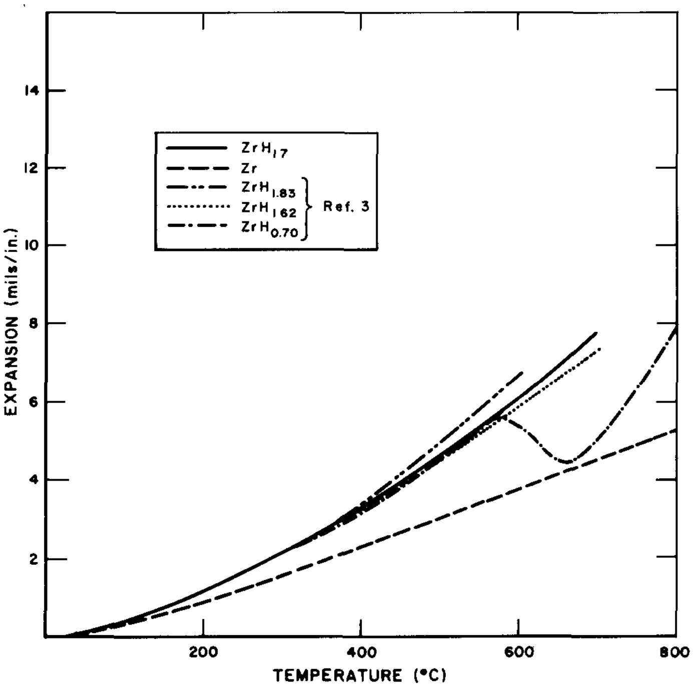

Figure 3. Thermal Expansion of Zirconium and Zirconium Hydrides

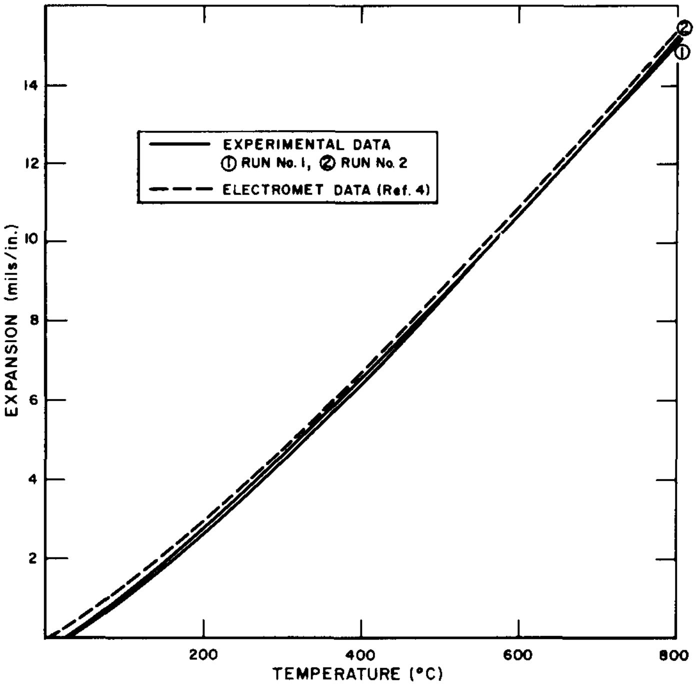

Figure 4. Thermal Expansion of Type 347 Stainless Steel

Figure 5 shows the thermal expansion curves for Hastelloy N, based on both the literature value[5] and present experimental data.

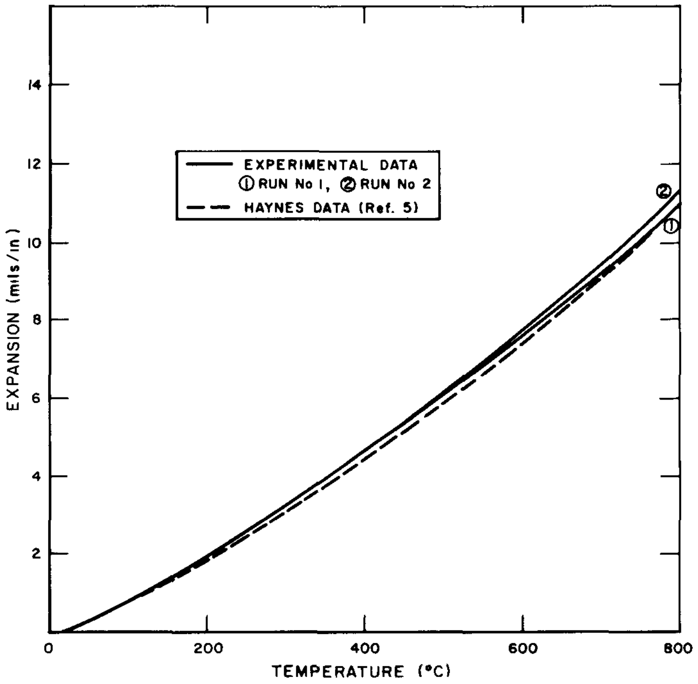

Figure 5. Thermal Expansion of Hastelloy N

Beryllium, originally selected as an axial reflector material within the fuel tube, and therefore in contact with the cladding, was also investigated. Experimental data from a series of four runs on actual SNAP reflector plugs are shown in Figure 6. For comparative purposes, data obtained from Brush Beryllium Corporation,[6] suppliers of SNAP beryllium, and from x-ray diffraction[7] are shown to bracket the experimental data.

Beryllium oxide, selected to replace the axially positioned beryllium reflectors, has been investigated on another project at Atomics International.[8] Expansion of the BeO is less than any of the materials in the SNAP fuel element, being approximately 25% lower than the fueled hydride material.

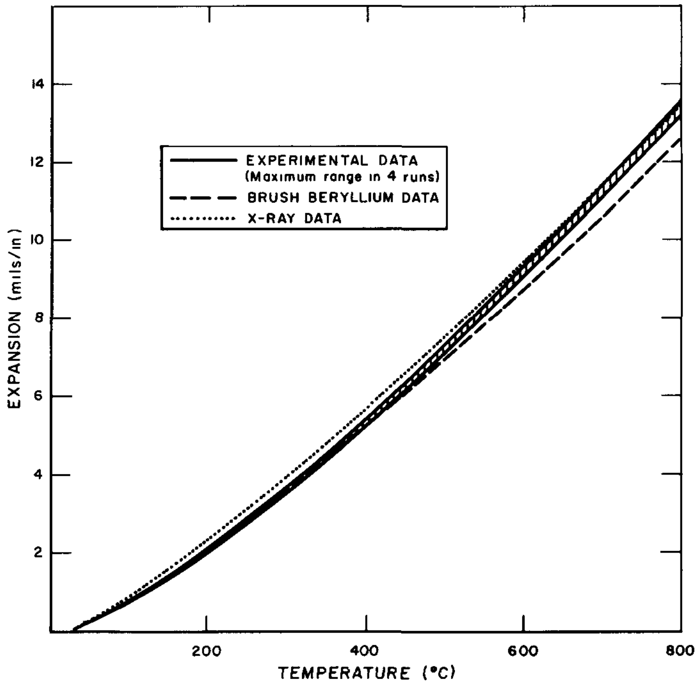

Figure 6. Thermal Expansion of Beryllium

V. ERROR ANALYSIS

A variety of factors are involved which introduce errors into the experimental data. The LVDT linearity is described by the manufacturer as being better than ± 1%, but utilization of calibration fixtures attached to the thermal expansion apparatus normally resulted in a reproducible accuracy of better than ± 0.5%, over the entire chart range. Full-scale chart range was normally set at 20 mils expansion, for most runs. Readability on the chart is better than 0.2%, thus the expansion is known to ±0.5% [in actual units, ±0.00005 in./in. (50 μ in./in.)] at full scale.

Temperature readings are highly susceptible to errors. Calibrated Chromel-Alumel thermocouples were usually reliable to ±1/2% of temperature recorded. Recorders have an inherent accuracy of approximately 1/2% of full scale, giving an expected overall accuracy of ± 1%. As a temperature standard, Armco iron has a sharp transformation at 910°C. During experimental runs, this transformation was always observed in the range of 908 to 912°C, indicating that recorder temperatures were normally accurate within ± 2°C at that temperature.

During initial calibration experiments using differential thermocouple techniques within the interior of a sample <u>vs</u> the normally used thermocouple, deviations of 5 to 10°C were observed in the region of 200°C, due to a specimen heating lag. This thermal lag was caused by low heat transfer characteristics of the system in this temperature region. Above this temperature, the deviation became less; and, above 400°C, the thermal lag was less than 1°C.

Calibration checks, with Armco iron and quartz, showed that the only correction factor required in the calculations was that introduced by the quartz adjacent to the specimen. The observed specimen expansion was lower than the true expansion by the amount of the quartz expansion. When a quartz sample was placed in the system, its observed expansion was -0.00001 ± 0.00001 in./in. at all temperatures in the range from room temperature to 1000°C, thereby allowing use of the thermal expansion of quartz as the correction factor, as the system errors were smaller than normal readability. Variations in values reported in the literature for the thermal expansion of Armco iron, particularly above 600°C, negate the use of Armco as a primary expansion standard.

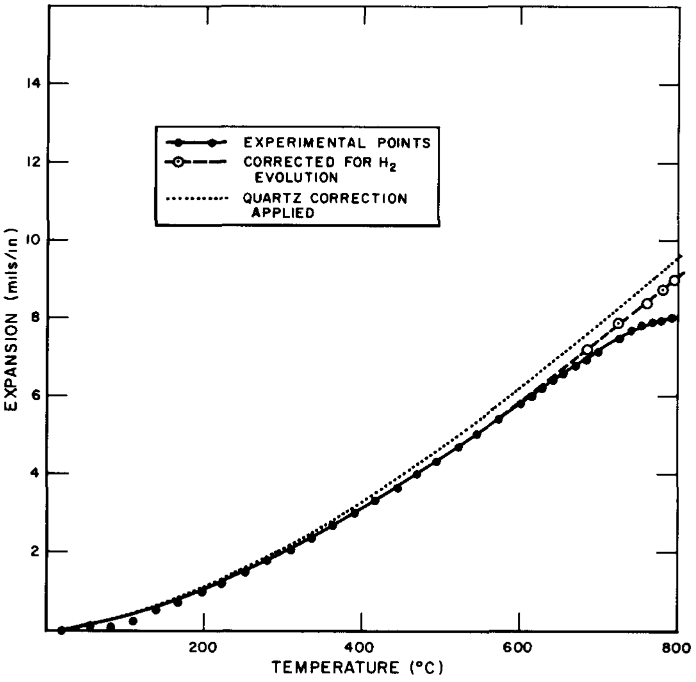

Figure 7. Thermal Expansion of Sample R-21
(Zr - 7 wt % U, H/Zr = 1.80, 9-19-60)

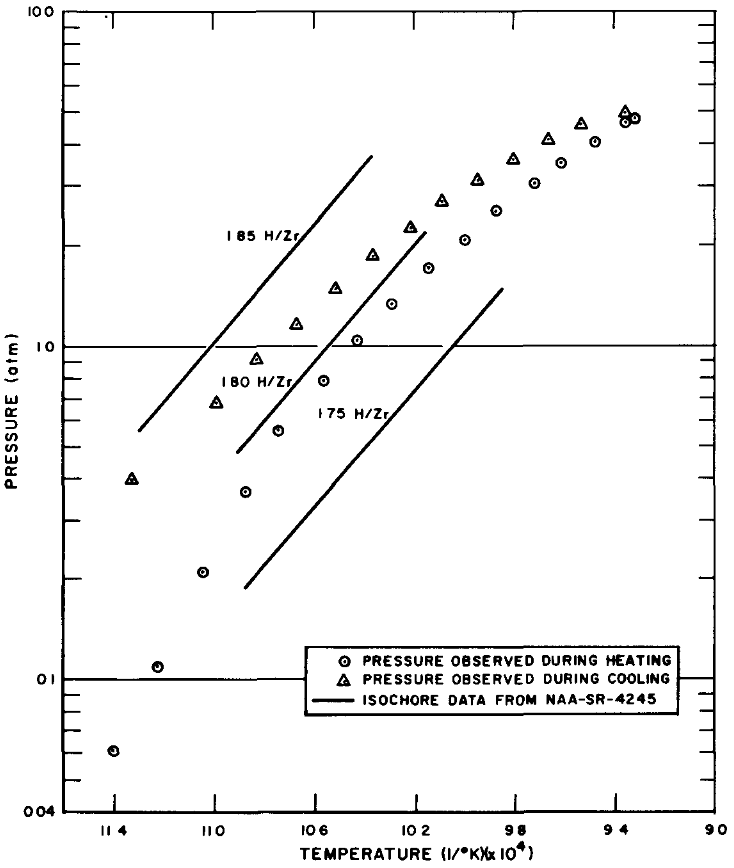

Figure 8. Dissociation Pressure of Sample R-21
(Zr - 7 wt % U, H/Zr = 1.80, 9-19-60)

Low temperature deviations in expansion were observed in all materials, due to the aforementioned temperature lag of the specimen at temperatures less than approximately 250°C. High temperature expansion deviations were observed on the hydrides, due to hydrogen loss from the specimen into the 34 cc void volume of the apparatus. In the composition range of H/Zr from 1.55 to 1.85, Zr - 7 wt % U hydrides contract at the rate of 10^{-2} in./in.H/Zr. Knowing the sample weight, dissociation pressure, and void volume of the apparatus, it is possible to apply this correction to the Zr-U hydrides. The resultant thermal expansion curves, after correction for hydrogen evolution, show upward concavities at all temperatures; whereas, without correction, contractions become evident only at high temperatures.

Figure 7 shows both the low and high temperature deviations observed in a typical thermal expansion run on hydrided material. Figure 8 shows the dissociation pressure over the specimen, as a function of temperature, during the same typical experimental run. Due to the system being dynamic in nature, equilibrium pressures are never obtained over the sample. However, by plotting both heating and cooling pressures, the equilibrium pressure can be assumed to be somewhere in between. By plotting these pressures on an isochore map, the method becomes an analytical tool to determine the approximate sample composition.

Reproducibility of the expansion data for all materials was always better than ± 1/2%, with less than ± 1/2% achieved in four consecutive runs of the same hydride material.

Curves were calculated by using a least squares analytical technique. A sample calculation is illustrated in Appendix II. Using the derived equations for calculating expansion at various temperatures, values were within ± 1% of the experimental curves, except at low temperatures.

VI. DATA COMPARISON

A comparison of the data obtained during this experimental program is plotted in Figure 9. Type 347 stainless steel expands at a rate greater than beryllium, Hastelloy N, and zirconium-uranium hydride. Table I, in Appendix II, lists the coefficients for the derived thermal expansion equation, as well as the coefficients for expansion from room temperature to 1000, 1200, and 1400°F. The coefficient (a) is a relative measure of low temperature deviation from the calculated curve. The coefficient (b) may be regarded as the room temperature thermal expansion coefficient, while coefficient (c) is the temperature dependent coefficient. In cases where (c) is small, the coefficient of thermal expansion changes only slightly as a function of temperature, as shown by the stainless steel; while larger values of (c) cause an upward concavity, as best illustrated by the zirconium-uranium hydride.

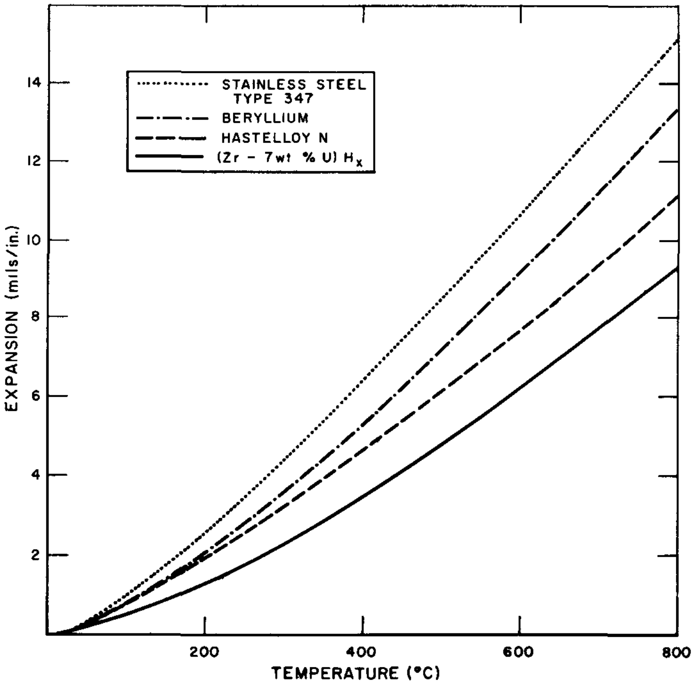

Figure 9. Thermal Expansion of SNAP Materials

In the temperature range investigated, all structural materials have thermal expansion coefficients greater than zirconium-uranium hydride. Part of this differential thermal expansion is eliminated during heating and normal reactor operation, due to the fact that the fuel is hotter than the cladding.

VII. SUMMARY

Data obtained during this experimental program for SNAP materials have been compared to the literature, where available, and found to correspond within normally expected experimental accuracy. Thermal expansion coefficients obtained for the temperature range of room temperature to 1200°F are: 10.34 x 10^{-6} in./in.-°F, for Type 347 stainless steel; 7.46 x 10^{-6} in./in.-°F, for Hastelloy N; 9.07 x 10^{-6} in./in.-°F, for beryllium; and 6.12 x 10^{-6} in./in.-°F, for zirconium-uranium hydride with an $N_H = 6.4$. Instantaneous thermal expansion coefficients, for any temperature from 200 to 1300°F, may be calculated from derived equations, for use in reactor analysis.

APPENDIX I

LEAST SQUARES METHOD OF SOLUTION FOR THERMAL EXPANSION DATA

Let:

Y = Expansion from room temperature to t°C (mils/in.)

X = Temperature (°C x 10^{-2})

$$Y = a + bX + cX^2$$

$$\text{I.}\quad \Sigma(Y) = Na + b\Sigma(X) + c\Sigma(X^2)$$

$$\text{II.}\quad \Sigma(XY) = a\Sigma(X) + b\Sigma(X^2) + c\Sigma(X^3)$$

$$\text{III.}\quad \Sigma(X^2Y) = a\Sigma(X^2) + b\Sigma(X^3) + c\Sigma(X^4)$$

For a standard expansion run which covers the range from room temperature up to 700 to 900°C, it is convenient, from a calculation standpoint, to use 100 to 700°C for a solution.

For a standard solution (100 to 700°C):

$$N = 7,\ \Sigma(X) = 28,\ \Sigma(X^2) = 140,\ \Sigma(X^3) = 784,\ \Sigma(X^4) = 4676$$

Fitting summations of X into Equations I to III:

$$7a + 28b + 140c = \Sigma(Y) \qquad \ldots(1)$$

$$28a + 140b + 784c = \Sigma(XY) \qquad \ldots(2)$$

$$140a + 784b + 4676c = \Sigma(X^2Y) \qquad \ldots(3)$$

Dividing through to obtain a:

$$(1) \div 7:\ a + 4b + 20c = \Sigma(Y)/7 \qquad \ldots(4)$$

$$(2) \div 28:\ a + 5b + 28c = \Sigma(XY)/28 \qquad \ldots(5)$$

$$(3) \div 140:\ a + 5.6b + 33.4c = \Sigma(X^2Y)/140 \qquad \ldots(6)$$

Eliminating a:

$$(5)-(4):\ b + 8c = \Sigma(XY)/28 - \Sigma(Y)/7 \qquad \ldots(7)$$

$$(6)-(5):\ 0.6b + 5.4c = \Sigma(X^2Y)/140 - \Sigma(XY)/28 \qquad \ldots(8)$$

Eliminating b:

$$(8) \times 5/3:\ b + 9c = \frac{5}{3}\left[\Sigma(X^2Y)/140 - \Sigma(XY)/28\right] \qquad \ldots(9)$$

$$(9)-(7):\ c = \frac{5}{3}\left[\Sigma(X^2Y)/140 - \Sigma(XY)/28\right] - \left[\Sigma(XY)/28 - \Sigma(Y)/7\right] \qquad \ldots(10)$$

Substituting c in (7) or (9), b is obtained.

Substituting b and c in (4), (5), or (6), a is obtained.

Substituting for X and Y:

$$\text{Expansion} = \frac{\Delta\ell}{\ell} = a \times 10^{-3} + b \times 10^{-5} t + c \times 10^{-7} t^2$$

where:

t is in °C, in the range of 100 to 700°C

a, b, and c are the derived coefficients

$\frac{\Delta\ell}{\ell}$ is in in./in.

APPENDIX II

SAMPLE SOLUTION FOR THERMAL EXPANSION

t (°C)	X	X^2	X^3	X^4	$\frac{\Delta \ell}{\ell}$ (mil/in.) Y	XY	X^2Y
100	1	1	1	1	0.44	0.44	0.44
200	2	4	8	16	1.22	2.44	4.88
300	3	9	27	81	2.22	6.66	19.98
400	4	16	64	256	3.38	13.52	54.08
500	5	25	125	625	4.70	23.50	117.50
600	6	36	216	1296	6.12	36.72	220.32
700	7	49	343	2401	7.65	53.55	374.85
Σ	28	140	784	4676	25.73	136.83	792.05

$$7a + 28b + 140c = 25.73 \qquad \ldots(1)$$

$$28a + 140b + 784c = 136.83 \qquad \ldots(2)$$

$$140a + 784b + 4676c = 792.05 \qquad \ldots(3)$$

$$(1) \div 7: \ a + 4b + 20c = 3.67571 \qquad \ldots(4)$$

$$(2) \div 28: \ a + 5b + 28c = 4.88680 \qquad \ldots(5)$$

$$(3) \div 140: \ a + 5.6b + 33.4c = 5.65750 \qquad \ldots(6)$$

$$(5)-(4): \ b + 8c = 1.21109 \qquad \ldots(7)$$

$$(6)-(5): \ 0.6b + 5.4c = 0.77070 \qquad \ldots(8)$$

$$(8) \times 5/3: \ b + 9c = 1.28450 \qquad \ldots(9)$$

$$
\begin{aligned}
(9)-(7):\ c &= 0.07341\\
b &= 1.21109 - 8(0.07341)\\
&= 0.62381\\
a &= 3.67571 - 4(0.62381) - 20(0.07341)\\
&= -0.28773
\end{aligned}
$$

$$\frac{\Delta \ell}{\ell}(\text{in./in.}) = -2.88 \times 10^{-4} + 6.24 \times 10^{-6}\ t + 7.34 \times 10^{-9}\ t^2$$

Check for solution of sample:

t (°C)	Original Exp. (mil/in.)	a	bt	ct^2	$a+bt+ct^2$ (mil/in.)	Deviation from Original
100	0.44	-0.288	0.624	0.073	0.41	-0.03
200	1.22	-0.288	1.248	0.294	1.25	+0.03
300	2.22	-0.288	1.872	0.661	2.24	+0.02
400	3.38	-0.288	2.496	1.174	3.38	0
500	4.70	-0.288	3.120	1.835	4.67	-0.03
600	6.12	-0.288	3.744	2.642	6.10	-0.02
700	7.65	-0.288	4.368	3.597	7.68	+0.03

TABLE I

THERMAL EXPANSION OF SNAP MATERIALS

	Type 347 S.S.	Hastelloy N	Be	Zr - 7 wt % U H/Zr 1.8
Constants in Equation (1)*				
$-a(\times 10^{1})$	6.34	3.94	4.78	2.88
$b(\times 10^{3})$	16.11	11.13	11.76	6.24
$c(\times 10^{6})$	4.52	3.87	7.19	7.34
Calculated $\alpha_{400^\circ C}^{\dagger} \left(\frac{\text{in.}}{\text{in.} - ^\circ C}\right) (\times 10^{6})$	19.73	14.22	17.51	12.11
Average Expansion $\left(\frac{\text{in.}}{\text{in.} - ^\circ C}\right) (\times 10^{6})$				
25 to 500°C	17.9	13.0	15.2	10.1
25 to 600°C	18.6	13.4	15.9	10.8
25 to 700°C	19.1	13.8	16.7	11.5
Average Expansion $\left(\frac{\text{in.}}{\text{in.} - ^\circ F}\right) (\times 10^{6})$				
77 to 1000°F	10.05	7.19	8.53	5.63
77 to 1200°F	10.34	7.46	9.07	6.12
77 to 1400°F	10.66	7.78	9.47	6.56

*Equation (1): $\frac{\Delta \ell}{\ell} = a + bt + ct^2$

Where: t is in °C, in the range of 100 to 700°C

$\frac{\Delta \ell}{\ell} = 0$ at 25°C

a, b, c are derived coefficients

† $\alpha_{400^\circ C}$ Instantaneous coefficient of thermal expansion at 400°C

REFERENCES

1. J. B. Vetrano, "Delta Phase Zirconium Hydride as a Solid Phase Moderator," BMI-1243 (December, 1957)
2. P. S. Drennan, "Melting and Forming of SER Fuel Rods," NAA-SR-4762 (October, 1960)
3. "Proceedings of the Second Metal Hydrides Conference, held at Denver Research Institute,"LAR-6 (February, 1960)
4. American Iron and Steel Institute, New York (1957)
5. "Developmental Data on Hastelloy Alloy N" Haynes Stellite Company, Kokomo, Indiana (May, 1959)
6. "Beryllium Fabrication," Brush Beryllium Company, Cleveland, Ohio (October, 1958)
7. "Nuclear Engineering Data Sheet No. 4 Beryllium," Nuclear Engineering, 3 (January, 1958) p 9
8. R. E. Taylor, "Thermal Conductivity and Thermal Expansion of BeO at Elevated Temperatures," NAA-SR-4905 (July, 1960)